

# Reversing the Critical Casimir force by shape deformation

Giuseppe Bimonte,<sup>1,2</sup> Thorsten Emig,<sup>3</sup> and Mehran Kardar<sup>4</sup>

<sup>1</sup>*Dipartimento di Scienze Fisiche, Università di Napoli Federico II,  
Complesso Universitario MSA, Via Cintia, I-80126 Napoli, Italy*

<sup>2</sup>*INFN Sezione di Napoli, I-80126 Napoli, Italy*

<sup>3</sup>*Laboratoire de Physique Théorique et Modèles Statistiques,  
CNRS UMR 8626, Bât. 100, Université Paris-Sud, 91405 Orsay cedex, France*

<sup>4</sup>*Massachusetts Institute of Technology, Department of Physics, Cambridge, Massachusetts 02139, USA*  
(Dated: March 1, 2022)

The exact critical Casimir force between periodically deformed boundaries of a 2D semi-infinite strip is obtained for conformally invariant classical systems. Only two parameters (conformal charge and scaling dimension of a boundary changing operator), along with the solution of an electrostatic problem, determine the Casimir force, rendering the theory practically applicable to any shape and arrangement. The attraction between any two mirror symmetric objects follows directly from our general result. The possibility of purely shape induced reversal of the force, as well as occurrence of stable equilibrium points, is demonstrated for certain conformally invariant models, including the tricritical Ising model.

PACS numbers: 11.25.Hf, 05.40.-a, 68.35.Rh

Fluctuation-induced forces (FIF) are ubiquitous in nature [1]; prominent examples include van der Waals [2], and closely related Casimir forces [3, 4], originating from quantum fluctuations of the electromagnetic field. Thermal fluctuations in soft matter also lead to FIF, most pronounced near a critical point where correlation lengths are large [5, 6]. Controlling the sign of FIF (attractive or repulsive) is important to myriad applications in design and manipulation of micron scale devices. This has been achieved with judicious choice of materials in case of quantum electrodynamic (QED) Casimir forces [7], and with appropriate boundary conditions for critical FIF [8, 9].

The non-additive character of FIF has also prompted a quest for reversing the sign of Casimir forces solely by manipulation of shapes. The original impetus comes from the intriguing result by Boyer [10] for the modification of QED zero point energy by a spherical metal shell. The suggestion that this result may imply repulsion between two hemispheres was later ruled out by a general theorem for attraction between mirror symmetric shapes [11, 12]. There are indeed specific geometrical arrangements in which the normally attractive QED force in vacuum appears repulsive when constrained along a specific axis (e.g. [13]), but is unstable when moved off such axis. Indeed, a generalized Earnshaw's theorem for FIF in QED rules out the possibility of stable levitation (and consequently force reversals) in most cases [14].

Two dimensional (2D) membranes have provided yet another arena for investigation of FIF, mostly focused on interactions arising due to modifications of capillary fluctuations (see, e.g. [15, 16] and references therein). More recently, motivated by the possibility that the lipid mixtures composing biological membranes are poised at criticality [17, 18], it has been proposed that inclusions

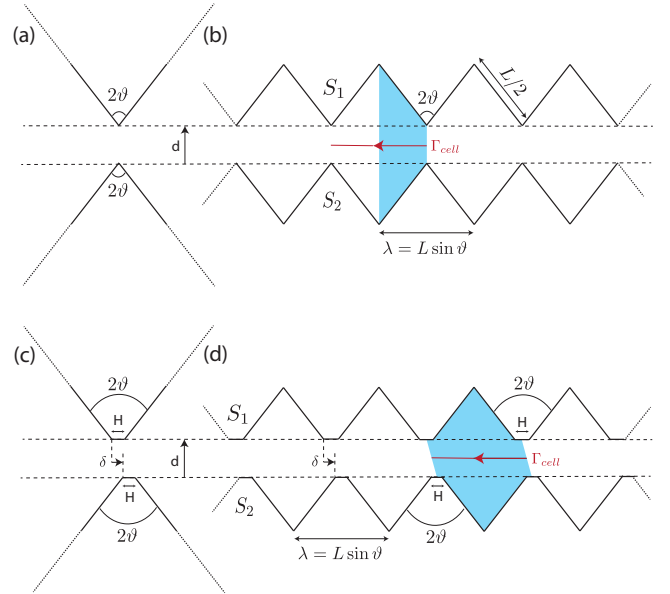


FIG. 1: Shapes considered: (a) two wedges, (b) strip with triangular corrugations, (c) truncated wedges with lateral shift, (d) strip with truncated corrugations and lateral shift. The blue regions mark half a unit cell (b) and a full unit cell (d).

(such as proteins) on such membranes are subject to 2D analogs of critical FIF [19]. A notable advantage is that 2D systems at criticality can be described by conformal field theories (CFT) [20, 21]: Casimir forces in a strip are related to the central charge of the CFT [22–24], with appropriate modification for boundaries. There are results for interactions between circles [19], needles [25]; Ref. [26] describes any compact shapes. Here, we consider the interaction between two wedges, or an array of wedges, as depicted in Fig. 1. We show that (with appro-

appropriate choice of CFT and boundary conditions) the FIF can be attractive or repulsive depending on the angle of the wedge; and that arrangements of stable equilibrium can be obtained with truncated wedges and arrays of them.

Consider two identically corrugated, infinite boundaries that enclose a critical classical medium (e.g., a fluid or magnetic system at its critical temperature  $T_c$ ) described by a CFT. The boundaries,  $S_1$  and  $S_2$ , impose conformally invariant boundary conditions  $a$  and  $b$ , respectively, on the medium. While our method is applicable to any shape, as specific examples we study the periodic, wedge-like shapes in Figs. 1(b,d). As interactions at proximity are dominated by the tips, we also consider the infinite wedges depicted in Figs. 1(a,c). Following our approach for compact shapes [26], the strip with deformed boundaries is conformally mapped to a flat strip. Information about the intervening medium enters only via its conformal charge  $c$ , and the scaling dimension  $h_{ab}$  of the boundary changing operator (BCO) from  $a$  to  $b$ ; with  $h_{ab} = 0$  for like boundaries [27]. All information about the shape of the deformed strip is encoded in the conformal map to the flat strip. This map, and hence the FIF, can be obtained from the solution to an electrostatic problem. In the following, we combine the normal ( $y$ ) and lateral ( $x$ ) components of the force into the complex expression  $F = (F_x - iF_y)/2$ . For periodically deformed boundaries with wavelength  $\lambda$  and length  $W \rightarrow \infty$ ,  $F = F_{\text{strip}} + F_{\text{geo}}$ , where the first contribution is the force on a strip, [37]

$$F_{\text{strip}} = -i \frac{\pi}{2} \left( \frac{c}{12} - \tilde{\eta} \right) \frac{W}{\lambda} \frac{1}{2\ell^2} \int_{\Gamma_{\text{cell}}} (\partial_z w)^2 dz, \quad (1)$$

that is determined by the free energy (per unit length)  $\mathcal{F}_{\text{strip}} = -(\pi/2)(c/12 - \tilde{\eta})/\ell$  of a flat strip of width  $\ell$ , and

$\tilde{\eta} \equiv 2h_{ab}$ . The second contribution is the geometric force

$$F_{\text{geo}} = -\frac{ic}{24\pi} \frac{W}{\lambda} \int_{\Gamma_{\text{cell}}} \{w, z\} dz, \quad (2)$$

where  $\{w, z\} \equiv (\partial_z^3 w / \partial_z w) - (3/2)(\partial_z^2 w / \partial_z w)^2$  is the Schwarzian derivative of the conformal map  $w(z)$  of the deformed to the flat strip [27]. Due to periodicity, it is sufficient to construct  $w(z)$  for a unit cell so that integrations in Eqs. (1,2) are restricted to a path  $\Gamma_{\text{cell}}$  that separates  $S_1$  and  $S_2$  within a unit cell [cf. Fig. 1]. Of course, the forces are proportional to the number of unit cells,  $W/\lambda$ . Whereas the strip force depends on shape simply via the electrostatic capacitance [26], the geometric force has a more intricate dependence on the boundary shapes. (The Schwarzian derivative vanishes if and only if  $w(z)$  is a global conformal map.)

Conformal maps are physically realized as equipotential curves and stream lines in electrostatics. We employ this analogy to derive a general result for the Casimir force in terms of the electrostatic potential  $U(x, y)$  on the strip with the two boundaries held at a fixed potential difference  $\Delta U = 1$ . The conformal map is then given by  $w(z) = U + iV$  where  $V$  is the conjugate harmonic function to  $U$ . Clearly  $\ell = \Delta U = 1$ . Since Eqs. (1,2) involve only derivatives of  $w(z)$ , we use the Cauchy-Riemann equations to get  $\partial_z w = \partial_x U - i\partial_y U$  and eliminate  $V$ . For practical computations (e.g. using finite element solvers) it is useful to express the Casimir force in terms of line integrals of real valued vector fields that are fully determined by derivatives of  $U$ . Parametrizing the contour  $\Gamma_{\text{cell}}$  by  $\mathbf{r}(s) = [x(s), y(s)]$  for  $0 \leq s \leq 1$ , and splitting into real and imaginary parts, we obtain the force in terms of  $c$ ,  $\tilde{\eta}$  and  $U$  as

$$F_{\text{strip}} = \frac{\pi}{2} \left( \frac{c}{12} - \tilde{\eta} \right) \frac{W}{\lambda} \left\{ \int_0^1 \mathbf{F}_1[\mathbf{r}(s)] \cdot \mathbf{r}'(s) ds + i \int_0^1 \mathbf{F}_2[\mathbf{r}(s)] \cdot \mathbf{r}'(s) ds \right\} \quad (3)$$

$$F_{\text{geo}} = -\frac{ic}{24\pi} \frac{W}{\lambda} \left\{ \int_0^1 \mathbf{G}_1[\mathbf{r}(s)] \cdot \mathbf{r}'(s) ds + i \int_0^1 \mathbf{G}_2[\mathbf{r}(s)] \cdot \mathbf{r}'(s) ds \right\} \quad \text{with the vector fields} \quad (4)$$

$$\mathbf{F}_1 = \left( \frac{-\partial_x U \partial_y U}{\frac{1}{2}((\partial_x U)^2 - (\partial_y U)^2)} \right), \quad \mathbf{F}_2 = \left( \frac{-\frac{1}{2}((\partial_x U)^2 - (\partial_y U)^2)}{-\partial_x U \partial_y U} \right) \quad (5)$$

$$\mathbf{G}_1 = \frac{1}{((\partial_x U)^2 + (\partial_y U)^2)^2} \left( \frac{\frac{1}{2}(\partial_x^2 U \partial_y U - \partial_x \partial_y U \partial_x U)^2 - \frac{1}{2}(\partial_x^2 U \partial_x U + \partial_x \partial_y U \partial_y U)^2}{(\partial_x^2 U \partial_x U + \partial_x \partial_y U \partial_y U)(\partial_x^2 U \partial_y U - \partial_x \partial_y U \partial_x U)} \right) \quad (6)$$

$$\mathbf{G}_2 = \frac{1}{((\partial_x U)^2 + (\partial_y U)^2)^2} \left( \frac{-(\partial_x^2 U \partial_x U + \partial_x \partial_y U \partial_y U)(\partial_x^2 U \partial_y U - \partial_x \partial_y U \partial_x U)}{\frac{1}{2}(\partial_x^2 U \partial_y U - \partial_x \partial_y U \partial_x U)^2 - \frac{1}{2}(\partial_x^2 U \partial_x U + \partial_x \partial_y U \partial_y U)^2} \right). \quad (7)$$

We note that the strip force  $F_{\text{strip}}$  is proportional to the

usual electrostatic force. This result also implies that the

critical Casimir force between any pair of mirror symmetric boundaries is attractive for  $c > 0$  [11, 12]: In this case the electrostatic potential must be constant along the  $x$ -axis of mirror symmetry. Choosing this axis as  $\Gamma_{\text{cell}}$  gives  $\mathbf{r}'(s) \sim -\hat{\mathbf{x}}$  and hence shows that both  $F_{\text{strip}}$  and  $F_{\text{geo}}$  have a vanishing real part and a negative imaginary part for  $c/12 - \tilde{\eta} > 0$ , which includes like boundaries ( $\tilde{\eta} = 0$ ). This implies a vanishing lateral force and positive normal force that corresponds to attraction in our notation.

Due to the simplicity of the related electrostatic problem, virtually any boundary shape can be studied by computing  $U$  either analytically (e.g. using the Schwarz-Christoffel (SC) map for polygons [28]), or numerically (using finite element solvers). Here we consider a simple profile composed of a periodic array of (truncated) wedges as in Figs. 1(b,d). For the triangular corrugations in Fig. 1(b), the SC map yields an analytic result for the force in terms of a single parameter implicitly determined in terms of  $\vartheta$  and  $L/d$ . Due to lack of space, we delegate the full solution to a forthcoming work, and study here short and large distances  $d$  only. At small  $d \ll L$ , the force is the sum of the contributions from the tips of the wedges, such that the normal force  $F_y = (W/\lambda)F_{\text{wedges},y}$ . The FIF between two infinite wedges of opening angle  $2\vartheta$  [Fig. 1(a)] is proportional to  $1/d$  on dimensional grounds, and given by

$$F_{\text{wedges},y} = c \left[ \left( \frac{1}{12} - \frac{\tilde{\eta}}{c} \right) \frac{\pi}{\pi - 2\vartheta} + \frac{1}{24} \frac{\pi - 2\vartheta}{\pi - \vartheta} \right] \frac{1}{d}, \quad (8)$$

where the first term corresponds to  $F_{\text{strip}}$  and the second to  $F_{\text{geo}}$ . The amplitude of this force is shown in Fig. 2 for different values of  $\tilde{\eta}/c$ , corresponding to unlike boundary conditions ( $\tilde{\eta} > 0$ ). Interestingly, for  $\tilde{\eta}/c < 1/8$  the force becomes attractive below a critical opening angle  $\vartheta$  [38]. This is different from the asymptotic large distance force between the boundaries,  $F_y = (\pi/2)(c/12 - \tilde{\eta})W/d^2$ , which is repulsive for  $\tilde{\eta}/c > 1/12$ . Hence, there is a reversal of the force between triangular corrugations from repulsive to attractive with decreasing separation  $d$  if

$$\frac{1}{12} < \frac{\tilde{\eta}_{(ab)}}{c} = \frac{2h_{(ab)}}{c} < \frac{1}{8}, \quad (9)$$

and  $\vartheta$  is sufficiently small. This is confirmed by our full analytic solution at all distances which is shown in the inset of Fig. 2 for different opening angles and a BCO of the tricritical Ising model that obeys Eq. (9). The change of sign corresponds to an *unstable* point.

However, these results together with the expected validity of the proximity force approximation (PFA) at very short separations suggest the possibility of a stable point if the tips of the wedges are truncated and replaced by plateaus of width  $H \ll L$ , as in Fig. 1(d). Indeed, for a single pair of truncated wedges [Fig. 1(c)], PFA at short distances  $d \ll H$  suggests

$$F_{\text{tr. wedges},y}^{\text{PFA}} = \frac{\pi}{2} \left( \frac{c}{12} - \tilde{\eta} \right) \frac{H}{d^2}, \quad (10)$$

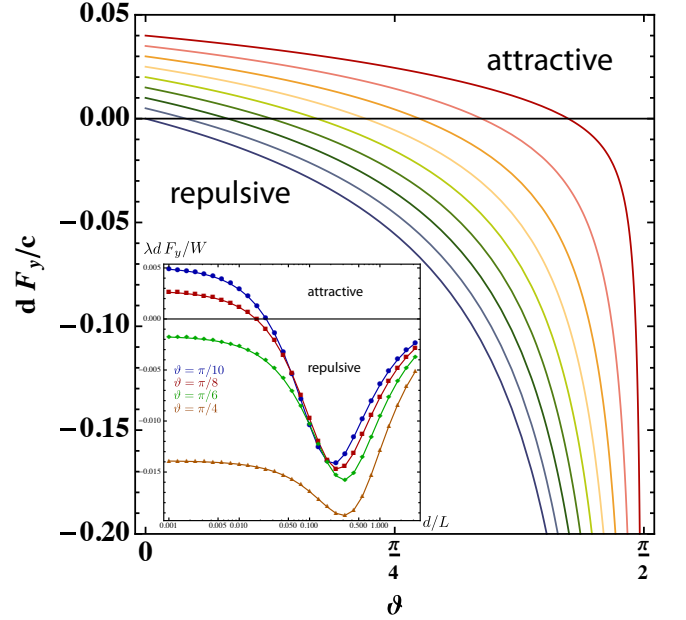


FIG. 2: Rescaled normal force  $F_y \sim 1/d$  between two infinite wedges as function of half opening angle  $\vartheta$ . The curves correspond to equidistant CFT parameter ratios  $\tilde{\eta}/c$  in the relevant interval  $1/12$  (red) to  $1/8$  (blue). Inset: Rescaled force between triangular corrugations at selected opening angles for the tricritical Ising model and boundary changing operator  $p = q = 2$  with  $\tilde{\eta}/c = 3/28 = 0.1071$  (see text for details).

which is repulsive for  $\tilde{\eta}/c > 12$ . At distances  $d \gg H$ , the plateaus become irrelevant, and the force approaches the result of Eq. (8). Hence two truncated wedges must have a stable point at intermediate distance if Eq. (9) holds and the opening angle is sufficiently small. This expectation is confirmed by an exact computation (using a SC map) of the normal and lateral force between two truncated wedges with lateral shift  $\delta$  [see Fig. 1(c)]. We additionally confirm that this configuration is stable with respect to displacements in the lateral direction.

Combining the above findings, for the truncated triangular corrugations of Fig. 1(d) we expect under the condition (9) and for sufficiently small  $\vartheta$  a stable equilibrium point (in both directions), and a saddle point at larger separations. For this geometry, a SC transformation can be performed in principle, but has to be evaluated numerically (which is cumbersome for a finite lateral shift  $\delta$ ). Hence, we employ the analogy to electrostatics as described by Eqs. (3,4). The electrostatic potential is computed by a finite element solver (FES) and subsequently the resulting vector fields [see Eqs. (5-7)] are integrated along the contour  $\Gamma_{\text{cell}}$ . To be specific, we chose the unitary CFT with conformal charge  $c = 7/10$  that describes the tricritical Ising model (TIM) and chose boundary conditions that are connected by the BCO with scaling dimension  $h_{ab} = 3/80$  so that condition in Eq. (9) is fulfilled. (The reason for these particular

choices shall become clear below when we discuss possible CFT's.) The accuracy of the FES can be established by comparing its results to those from a SC transformation for vanishing lateral shift  $\delta$ . The results of both methods for the normal force (acting on the lower boundary  $S_2$ ) between truncated triangular corrugations with  $\vartheta = \pi/10$  are shown in Fig. 3. The agreement is excellent and confirms sufficient accuracy of the FES. The normal force shows the expected sign reversals from repulsive to attractive and back to repulsive. For a finite lateral shift  $\delta$  we used the FES to compute both normal and lateral force. The lateral force at a normal distance close to the stable point ( $d/H = 3.4$ ) is plotted in the inset of Fig. 3, demonstrating mechanical stability also in the lateral direction. The global force field and curves of constant Casimir potential are shown in Fig. 4. The presence of a stable equilibrium point, and a saddle point, (both at  $\delta = 0$ ) is clearly confirmed.

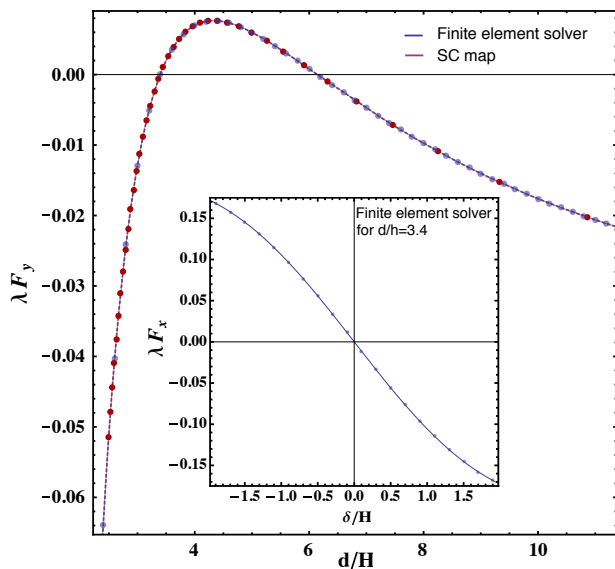


FIG. 3: The normal Casimir force acting on boundary ( $S_2$ ) for vanishing lateral shift  $\delta$ , as function of separation  $d$  for the geometry of Fig. 1(d) with  $\vartheta = \pi/10$ . Parameters applicable to the tricritical Ising model with boundary changing operator of scaling dimension  $h_{2,2} = 3/80$  are used. Inset: The lateral Casimir force close to stable separation  $d = 3.4H$  as a function of the scaled lateral shift.

It is interesting to explore which critical systems allow for a stable equilibrium point in the above geometry. In the following, we identify unitary minimal CFT models with  $c < 1$  that permit boundary conditions consistent with the criteria in Eq. (9). For unitary models the conformal charge is restricted to the discrete values  $c = 1 - 6/[m(m+1)]$  with integer  $m \geq 2$ . The allowed scaling dimensions of the primary operators can assume

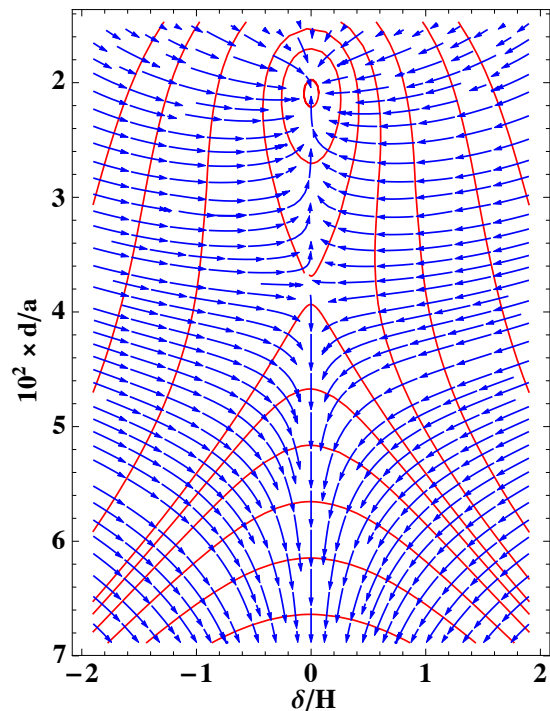


FIG. 4: Casimir force field and curves of constant Casimir potential as function of normal separation  $d$  and lateral shift  $\delta$ , for the same geometry and CFT as in Fig. 3. The saddle point, and the stable equilibrium point are clearly visible.

the values [20]

$$h_{p,q} = \frac{[(m+1)p - mq]^2 - 1}{4m(m+1)}, \quad (11)$$

with  $p = 1, 2, \dots, m-1$ , and  $q = 1, 2, \dots, p$ . Cardy has shown that all possible highest weight states with scaling dimension  $h_{p,q}$  may be realized by a BCO for an appropriate choice of boundary conditions ( $ab$ ) on the flat strip [29]. The two conformally invariant boundary conditions, or states that are connected by a BCO, are determined by the fusion rules for the two (bulk) primary fields that correspond to the boundary states. The condition of Eq. (9) can only be fulfilled for  $p = q$ . It turns out that for  $m = 3$  (Ising model),  $m = 5$  (3-state Potts model), and  $m = 7$  no primary operator obeys the condition. For all other models with  $m \leq 13$  there is exactly one operator whose dimension obeys the condition, while for  $m > 13$  two or more operators with suitable dimensions may exist. The simplest models with suitable BCO's are the TIM ( $m = 4$ ,  $c = 7/10$ ,  $h_{2,2} = 3/80$ ) and the tricritical 3-state Potts model ( $m = 6$ ,  $c = 6/7$ ,  $h_{3,3} = 1/21$ ). These considerations underlie our choice of the TIM for Figs. 3, 4. There are certainly other minimal models that also allow for conformally invariant boundary conditions that lead to a stable point.

Tricritical points are a common feature of many phase diagrams, corresponding to the point where a continu-

ous transition becomes first order, as can be observed by addition of vacancies or other impurities to an Ising magnet, or helium 3 to superfluid helium 4 (see, e.g. Ref. [30] for a review). Possible boundary conditions compatible with a renormalization group fixed point at tricriticality are discussed in Ref. [31]. Fusion rules in CFT [27] provide another route to characterizing conformally invariant boundary conditions. For the TIM with the BCO of scaling dimension  $h_{2,2} = 3/80$ , the relevant fusion rules are  $|1/10\rangle \times |7/16\rangle = |3/80\rangle$ ,  $|3/5\rangle \times |7/16\rangle = |3/80\rangle$ ,  $|3/2\rangle \times |3/80\rangle = |3/80\rangle$ ,  $|0\rangle \times |3/80\rangle = |3/80\rangle$ ,  $|1/10\rangle \times |3/80\rangle = |3/80\rangle + |7/16\rangle$ , and  $|3/5\rangle \times |3/80\rangle = |3/80\rangle + |7/16\rangle$ . The last two rules are relevant since for a semi-infinite strip the lowest dimension determines the free energy. Through appropriate choice of surface couplings and magnetic fields, the TIM admits the following conformally invariant boundary states [32, 33]: (i) A disordered state of free spins, corresponding to  $|7/16\rangle$ ; (ii) Maximally ordered (fixed) spins (+ or -), with  $|0\rangle$ ,  $|3/2\rangle$ . The phase transition between the above surface states can occur through (iii) Partially polarized (+ or - with vacancies) at finite surface fields, for  $|1/10\rangle$ ,  $|3/5\rangle$ ; or (iv) Through a so called degenerate point at zero surface field, with  $|3/80\rangle$ . The fusion rules show that a stable point with vanishing FIF can occur for the following combinations  $(a, b)$  of boundary conditions:

1. (fixed spin, degenerate),
2. (partially polarized, free spin),
3. (partially polarized, degenerate).

The stability of these boundary states (fixed points) with respect to a boundary magnetic field and spin couplings is determined by the boundary phase diagram of the TIM [33]. The free and fixed boundary conditions can be achieved relatively easily (at least in simulations), while the degenerate and partially polarized states require tuning one parameter (the surface coupling, or surface field). We expect that the combination of *partially polarized* and *free spin* conditions is the most promising candidate.

The conditions obtained here for the observation of a stable equilibrium point with FIF are rather restrictive. This demonstrates on the one hand the difficulty of achieving stability solely by FIF, on the one hand, and absence of its strict impossibility (ala Earnshaw [14]) on the other. For other examples in 2D, we could look for other realizations of CFT in interface (restricted solid-on-solid) models [34]. It would be quite interesting to explore the possibility of stability with critical FIF in three dimensions. It is not a priori clear if the necessary conditions in higher dimensions will be less or more restrictive. Since  $d = 3$  is the upper critical dimension for the TIM, at least in this case the question could in principle be resolved by generalizing standard field theory methods [31] to wedge/cone geometries [35, 36].

We thank R. L. Jaffe for valuable discussions. This research was supported by Labex PALM AO 2013 grant

CASIMIR, and the NSF through grant No. DMR-12-06323.

- 
- [1] M. Kardar and R. Golestanian, Rev. Mod. Phys. **71**, 1233 (1999).
  - [2] V. A. Parsegian, *Van der Waals Forces* (Cambridge University Press, 2005).
  - [3] H. B. G. Casimir, Proc. K. Ned. Akad. Wet. **51**, 793 (1948).
  - [4] M. Bordag, G. L. Klimchitskaya, U. Mohideen, and V. M. Mostepanenko, *Advances in the Casimir Effect* (Oxford University Press, 2009).
  - [5] P.-G. de Gennes and M. E. Fisher, C. R. Acad. Sci. Ser. B **287**, 207 (1978).
  - [6] M. Krech, *The Casimir effect in Critical systems* (World Scientific, 1994).
  - [7] J. Munday, F. Capasso, and V. Parsegian, Nature **457**, 170 (2009).
  - [8] F. Soyka, O. Zvyagolskaya, C. Hertlein, L. Helden, and C. Bechinger, Phys. Rev. Lett. **101**, 208301 (2008).
  - [9] C. Hertlein, L. Helden, A. Gambassi, S. Dietrich, and C. Bechinger, Nature **451**, 172 (2008).
  - [10] T. H. Boyer, Phys. Rev. **174**, 1764 (1968).
  - [11] O. Kenneth and I. Klich, Phys. Rev. Lett. **97**, 160401 (2006).
  - [12] C. P. Bachas, J. Phys. A: Math. Theor. **40**, 9089 (2007).
  - [13] M. Levin, A. P. McCauley, A. W. Rodriguez, M. T. H. Reid, and S. G. Johnson, Phys. Rev. Lett. **105**, 090403 (2010).
  - [14] S. J. Rahi, M. Kardar, and T. Emig, Phys. Rev. Lett. **105**, 070404 (2010).
  - [15] C. Yolcu, I. Z. Rothstein, and M. Deserno, Phys. Rev. E **85**, 011140 (2012).
  - [16] E. Noruzifar, J. Wagner, and R. Zandi, Phys. Rev. E **88**, 042314 (2013).
  - [17] S. L. Veatch, O. Soubias, S. L. Keller, and K. Gawrisch, PNAS **104**, 17650 (2007).
  - [18] T. Baumgart, A. T. Hammond, P. Sengupta, S. T. Hess, D. A. Holowka, B. A. Baird, and W. W. Webb, PNAS **104**, 3165 (2007).
  - [19] B. B. Machta, S. L. Veatch, and J. Sethna, Phys. Rev. Lett. **109**, 138101 (2012).
  - [20] D. Friedan, Z. Qui, and S. Shenker, Phys. Rev. Lett. **52**, 1575 (1984).
  - [21] J. L. Cardy, in *Fields, Strings, and Critical Phenomena*, edited by E. Brézin and J. Zinn-Justin (Elsevier, New York, 1989).
  - [22] J. Cardy, Nucl. Phys. B **275**, 200 (1986).
  - [23] P. Kleban and I. Vassileva, J. Phys. A: Math. Gen. **24**, 3407 (1991).
  - [24] P. Kleban and I. Peschel, Z. Phys. B **101**, 447 (1996).
  - [25] O. A. Vasilyev, E. Eisenriegler, and S. Dietrich, Phys. Rev. E **88**, 012137 (2013).
  - [26] G. Bimonte, T. Emig, and M. Kardar, EPL **104**, 21001 (2013).
  - [27] P. di Francesco, P. Mathieu, and D. Sénéchal, *Conformal Field Theory* (Springer, 1997).
  - [28] W. R. Smythe, *Static and dynamic electricity* (McGraw-Hill, 1950).
  - [29] J. L. Cardy, Nucl. Phys. B **324**, 581 (1984).

- [30] I. D. Lawrie and S. Sarbach, *Phase Transition and Critical Phenomena* (Academic, 1984), vol. 9, p. 1.
- [31] M. Krech and S. Dietrich, Phys. Rev. A **46**, 1886 (1992).
- [32] L. Chim, Int. J. Mod. Phys. A **11**, 4491 (1996).
- [33] I. Affleck, J. Phys. A: Math. Gen. **33**, 6473 (2000).
- [34] V. Pasquier, J. Phys. A: Math. Gen. **20**, 5707 (1987).
- [35] M. F. Maghrebi, S. J. Rahi, T. Emig, N. Graham, R. L. Jaffe, and M. Kardar, PNAS **108**, 6867 (2011).
- [36] M. F. Maghrebi, Y. Kantor, and M. Kardar, EPL **96**, 66002 (2011).
- [37] Throughout the paper we measure energies in units of  $k_B T_c$ .
- [38] The threshold  $\tilde{\eta}/c = 1/8$  corresponds to a free field theory ( $c = 1$ ) with mixed Dirichlet and Neumann boundary conditions.